Numerical Modeling of Recent Trans-Pacific Tsunami Recorded at Tide Gauges in Japan

by
Yuichiro Tanioka and Masami Okada

ABSTRACT

Numerical simulation of the trans-Pacific tsunami is examined for three large earthquakes (the 1996 Aleutian, 1995 Chile, and 1996 Irian Jaya earthquakes) occurred in the last two years. Overall, the observed and computed maximum tsunami heights at tide gauges in Japan show good agreements.

1. INTRODUCTION

In 1960, the tsunami from the Chilean earthquake propagated across the Pacific ocean and killed about 140 people in Japan. Since then, the trans-Pacific tsunami was studied extensively. In recent years, numerical modeling of trans-Pacific tsunami have been significantly developed (Goto et al, 1988, Imamura et al., 1990, etc.). However, these numerical methods have never examined by recent trans-Pacific tsunamis caused by large earthquakes. The fault parameters for those earthquakes can be reliably estimated using various data, such as seismic, geodetic, or near-field tsunami data..

In last two years, tsunamis from three large earthquakes (the 1995 Chile, 1996 Irian Jaya, and 1996 Aleutian earthquakes) propagated across the Pacific ocean and recorded at tide gauges in Japan. In this paper, we use those three earthquakes as test cases to examine the numerical method to compute the trans-Pacific tsunami. The fault parameters of the earthquakes are carefully estimated from the available data. The observed tsunami heights at tide gauges are compared with the computed heights.

2. METHOD

(1) Generation of Tsunami

The initial condition of tsunami is the water surface displacement caused by ocean bottom deformation due to faulting. The fault motion of the earthquake can be described by the fault parameters: the location of the fault, geometry (strike, dip, and rake), the fault size (length and width) and the slip amount. From these fault parameters, the ocean bottom deformation can be computed using Okada's (1985) equations.

(2) Computation of Tsunami Propagation

Atsunami which is generated by a large earthquake can be treated as a linear long wave because the wavelength is substantially larger than the water depth.

Seismology and Volcanology Department, Meteorological Research Institute, Tsukuba, 305 Japan

For tsunamis propagating a long distance such as across the Pacific ocean, the effects of Earth's sphericity and rotation (Coriolis force) must be also included. The integrated equations for linear long waves with the Coriolis force in the spherical coordinate system (longitude φ and latitude θ) are

$$\frac{\partial Q_\varphi}{\partial t} = -\frac{gd}{R\sin\theta}\frac{\partial h}{\partial \varphi} - fQ_\theta$$

$$\frac{\partial Q_\theta}{\partial t} = -\frac{gd}{R}\frac{\partial h}{\partial \theta} - fQ_\theta$$

$$f = 2\Omega\cos\theta$$

and

$$\frac{\partial h}{\partial t} = -\frac{1}{R\sin\theta}\left[\frac{\partial}{\partial\theta}(Q_\theta \sin\theta) + \frac{\partial Q_\varphi}{\partial\varphi}\right]$$

where R is the radius of the earth, g is the acceleration of gravity, d is water depth, Ω is the rotation vector of the earth, h is the height of the water displaced from equilibrium position, and Q is The flow rate. We solved the above equations using finite-difference calculations on a staggered grid system.

Further, the grid size on the entire Pacific Basin must be carefully chosen to make the effects of numerical and physical dispersion equal. Imamura et al., (1990) showed that the choice of the grid size can be evaluated using the Imamura number, *Im*, defined as

$$\mathrm{Im} = \Delta x \sqrt{1 - \left(C_0 \Delta t / \Delta x\right)^2} \Big/ 2h \qquad (2)$$

where Δx is the grid size, Δt is the time step, and $C_0 = \sqrt{gh}$. The value of *Im* must be about 1 to simulate the linear Boussinesq equation using the finite difference computation for a linear long wave. We chose the grid size (Δx) of 5 minutes and the time step (Δt) of 5 seconds to satisfy the stability condition of numerical computation. Using Equation (2) for the above case, Im is 1.15 in the N-S direction by assuming that the average depth is 4000m. In the E-W direction, Im varies with latitude and Im is 0.73-1.15 within the latitude between 50 and 0 degree. These results show that Im for the above case is about 1, so the 5 mitutes grid system on the Pacific Basin should make the numerical dispersion equal to the physical dispersion.

Near coastal area, the bathymetry changes rapidly and cannot be adequately represented by a 5 minutes grid (~ 10 km). Therefore, in the coastal area (near the west coast of North America, Aleutian, Hawaii, and Japan), 1 minutes grid (~ 2 km) spacing is used. In addition to that, 20 seconds grid (~ 600 m)spacing is used near some of the tide gauge stations in Japan.

3. THE 1996 ALEUTIAN EARTHQUAKE

The Aleutian earthquake of June 10, 1996 (Ms 7.6, Mw 7.9) occurred off the Delarof Islands, Alaska (Figure 1). The NEIS Preliminary Determination of Epicenters (PDE) provides the source parameters: origin time, 04:03:35.48 GMT; epicenter, 51.564°N, 177.588°W; magnitude, Ms 7.6. The focal mechanism of the earthquake from the Havard CMT indicates thrust type faulting with a shallow dip angle (20°) (Figure 1). It

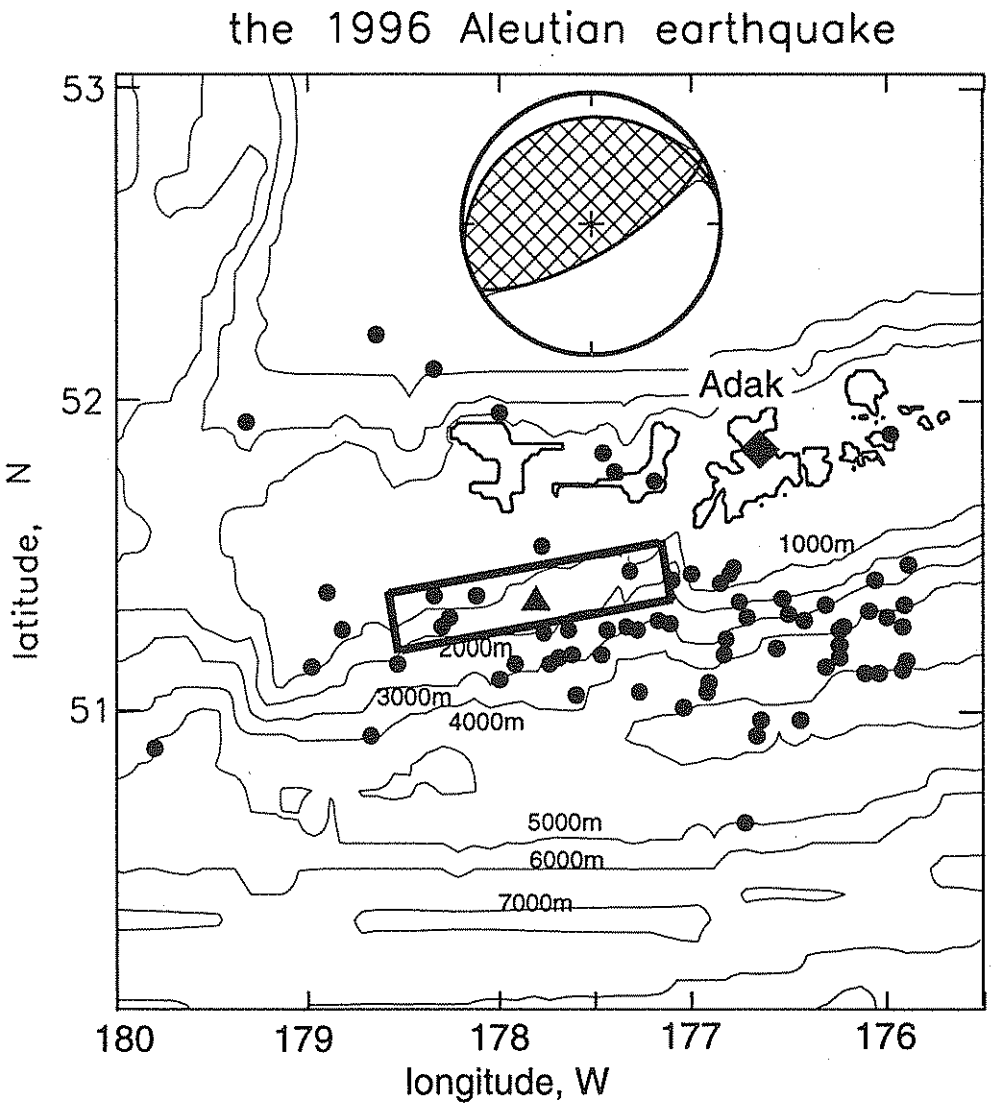

Figure 1. The focal mechanism and the best fault model of the 1996 Aleutian earthquake. A frame shows the best fault model. A triangle is the epicenter of the mainshock. Circles are the epicenter of aftershocks. Diamond shows the tide gauge (Adak).

generated trans-Pacific tsunamis which were recorded at tide gauge stations in the west coast of North America, Hawaii and Japan. The source time function of the earthquake was determined by the Michigan group (Tanioka and Ruff, 1997) using teleseismic body waves. It shows the duration of 54 seconds, the seismic moment of $7.3X10^{20}$ Nm and the depth of 18 km. No significant directivity was also observed.

There is one near-field tsunami waveform recorded at a tide gauge station, Adak, about 100 km away from the epicenter (Figure1). Using a pure thrust type fault (strike=260°, dip=20°, rake=90°) which is consistent with the focal mechanism, we computed the tsunami waveform at Adak for various fault sizes. The best fault model which

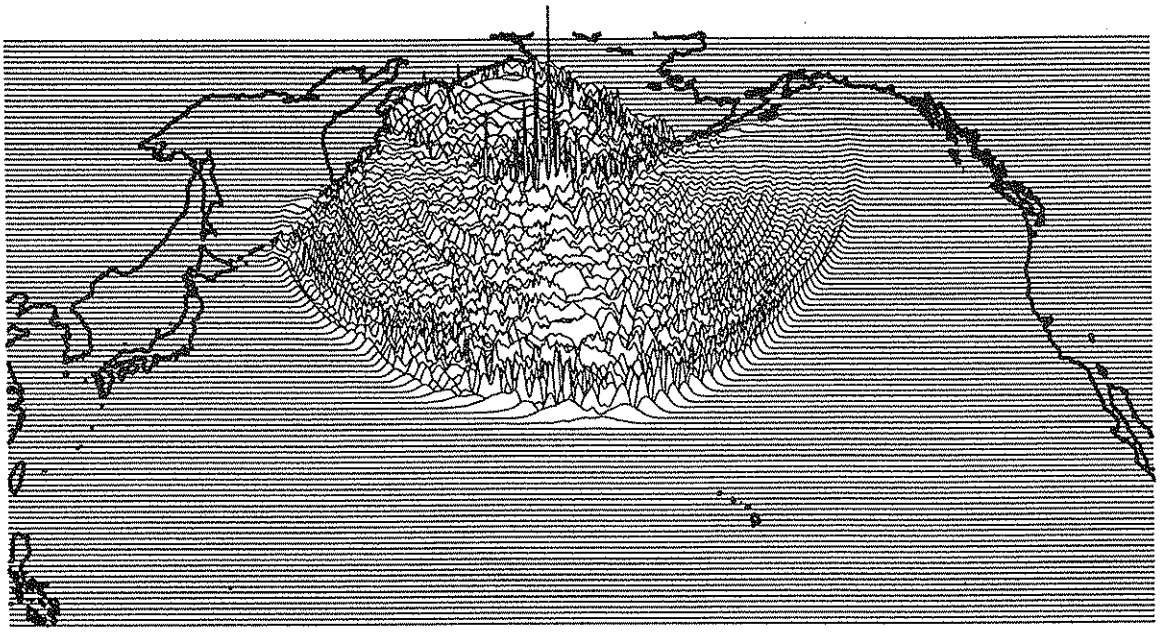

Figure 2. Snapshot of tsunami 3 hours after the 1996 Aleutian earthquake

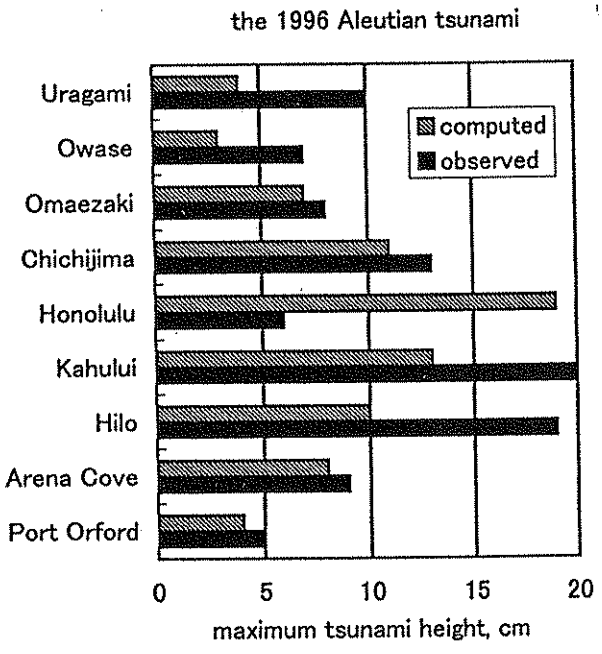

Figure 3. Comparison of observed and computed maximum tsunami heights at tide gauges in Japan, Hawaii, and west coast of North America.

explained the observed waveform well is shown in Figure 1 (length 110 km, width 20 km, slip 4 m). The epicenter is located near the center of the fault. This result and no significant directivity from the body wave analysis may suggest the bilateral rupture process of the 1996 Aleutian earthquake. Also, the rupture area is much smaller than the aftershock area (Figure 1). This may indicate that the moment release of the mainshock was concentrated in the asperity area..

Using this fault model, now we compute the trans-Pacific tsunami. Figure 2 shows the snapshot of tsunami propagation across the Pacific ocean 3 hours after the earthquake. As we can see in Figure2, large tsunamis propagate toward Hawaii, but very small tsunamis propagate toward the west coast of North America. This is due to the directivity effect; tsunami heights are usually smaller in the direction parallel to the orientation

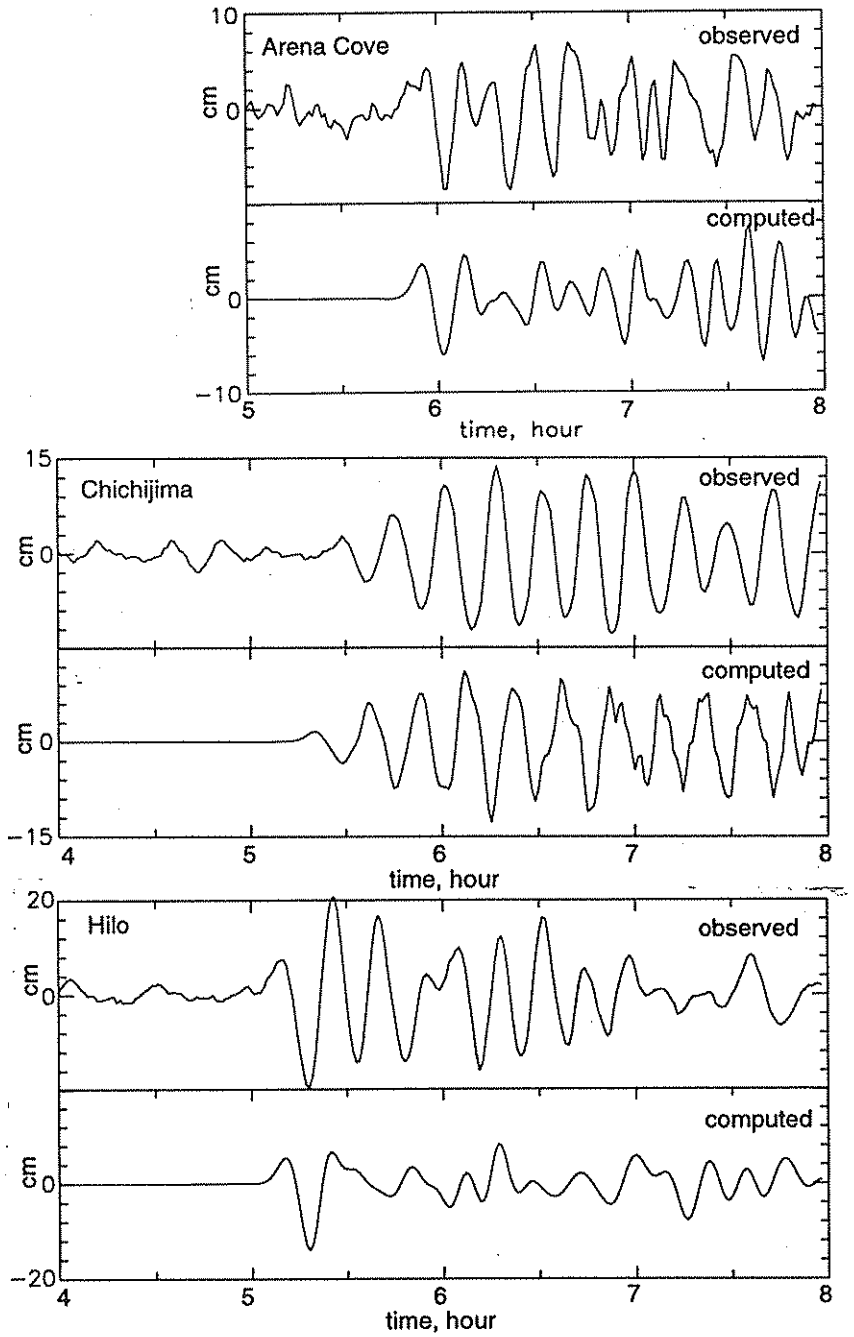

Figure 4. Comparison of observed and computed tsunami waveforms at three tide gauges.

(strike) of the fault (Ben-Menahem and Rosenman, 1977). Figure 3 compare the observed and computed maximum tsunami heights at the tide gauges in Japan (Uragami, Owase, Omaezaki, and Chichijma), Hawaii (Honolulu, Kafului, and Hilo), and the west coast of North America (Arena Cove and Port Orford). The maximum tsunami heights represent the largest tsunami heights during 3 hours from the first peak. The observed and computed maximum tsunami heights

fit well except at the Hawaiian stations. In Figure 4, we compared the observed and computed waveforms at three tide gauges. At Arena Cove and Chichijima, the observed and computed waveforms show the very good agreement, but not at Hilo. This may suggest that finer grid system or more accurate bathymetry near Hawaii is necessary to improve the accuracy of the model.

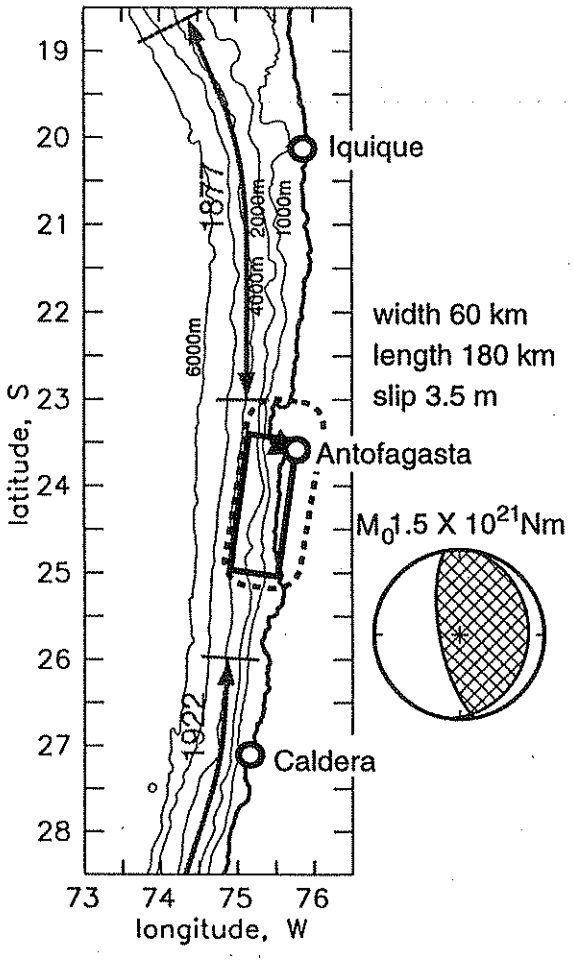

Figure 5. The best fault model and the focal mechanism of the 1995 Chile earthquake. A flame shows the best fault model. A star is the epicenter of the mainshock. Dashed ellipse shows the aftershock area. Circles are tide gauges.

4. THE 1995 CHILE EARTHQUAKE

The Chile earthquake of July 30, 1995 (Mw 8.0) occurred off Antofagasta, Northern Chile (Figure 5). The NEIS Preliminary Determination of Epicenters (PDE) provides the source parameters: origin time, 05:11:23.6 GMT; epicenter, 23.340°N, 70.294°W; magnitude, Ms 7.3. The focal mechanism of the earthquake (Ruegg et al., 1996) indicates thrust type faulting with a shallow dip angle (19°) (Figure 1). Ruegg et al., (1996) also determined three subevents from body wave analysis and suggested that the

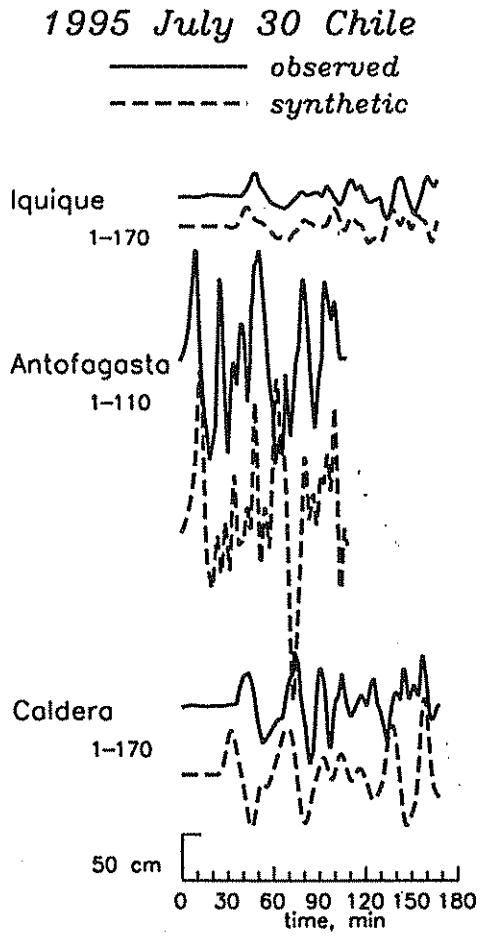

Figure 6. Comparison of the observed and computed tsunami waveforms

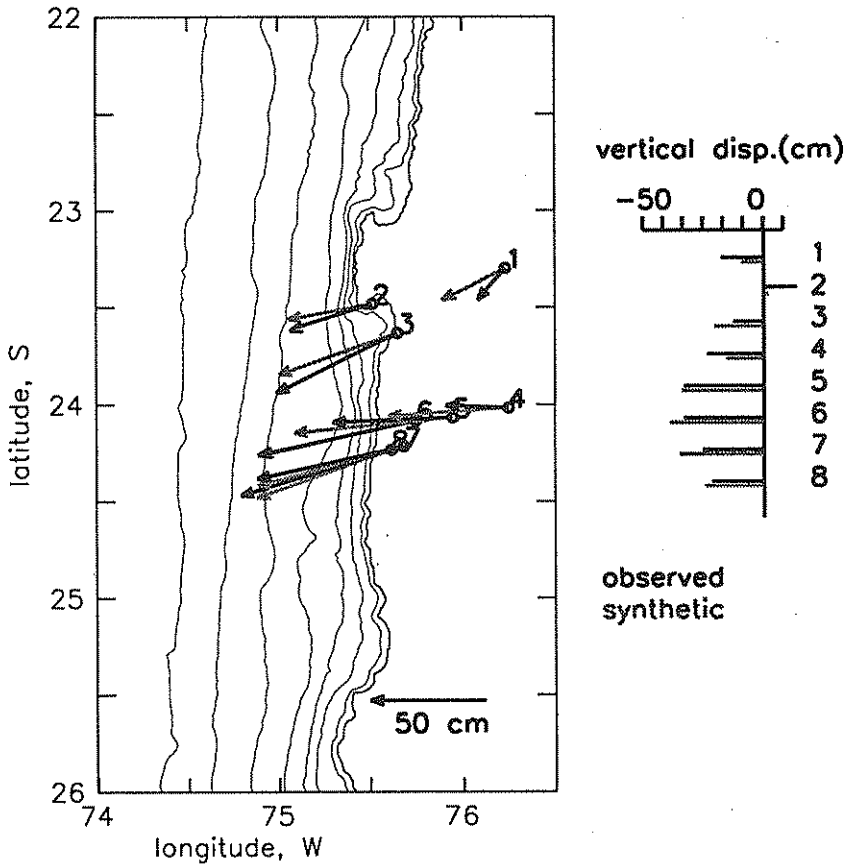

Figure 7. Comparison of the observed and computed coseismic displacement field. (left) Comparison of the horizontal displacements. (right) Comparison of the vertical displacements.

rupture propagated to southward, the fault length is about 180 km. The total seismic moment is estimated as 0.9 X 10^{21} Nm. They also determined the fault width of 60 km and slip of about 5m using the coseismic surface displacement field observed by the GPS network near the source region.

The 1995 Chile earthquake also generated large tsunamis. In addition to the coseismic displacement data (Ruegg et al., 1996), we used the tsunami waveforms recorded at three tide gauges in northern Chile (Figure 5) to determine the fault parameters. Using a thrust type fault (strike=8°, dip=20°, rake=107°), we computed the tsunami waveforms and the surface displacement field for various fault sizes and depths. The best fault model (length 180 km, width 60 km, slip 3.5 m) is shown in Figure 5. The depth of the down-dip edge of the fault is well-estimated as 40 km. Figure 6 shows the computed tsunami waveforms also fit well with the observed waveforms. Figure 7 shows that the computed surface displacement field is consistent with the observed field. The seismic moment is 1.5 X 10^{20} Nm by assuming that the rigidity 4 X 10^{10} N/m^2. This result is consistent with

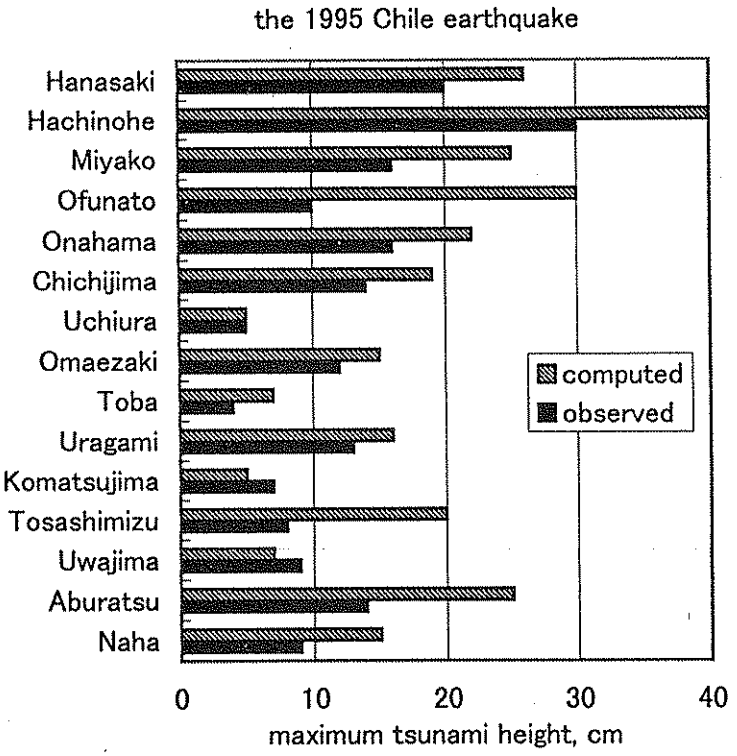

Figure 8. Comparison of the observed and computed maximum tsunami heights at tide gauges in Japan.

the estimate from the body wave analysis.

Tsunamis from the 1995 Chile earthquake propagated across the Pacific ocean and recorded at tide gauge stations in Japan. We computed the trans-Pacific tsunami using the above fault model which is well-determined by seismic, coseismic displacement, and near-filed tsunami data. .Figure 8 shows that the observed and computed maximum tsunami heights during 3 hours after the first arrival of tsunami at tide gauges in Japan. Computed maximum tsunami heights are slightly overestimated the observed maximum tsunami heights. More detail investigation is necessary to investigate this small differences.

5. THE 1996 IRIAN JAYA EARTHQUAKE

The Irian Jaya earthquake of February 17, 1996 (Mw 8.1) occurred off Biak Islands, Indonesia (Figure 10). The NEIS Preliminary Determination of Epicenters (PDE) provides the source parameters: origin time, 05:59:30.55 GMT; epicenter, 0.891°S, 136.952°E; magnitude, Ms 8.1. The focal mechanism of the earthquake from Harvard CMT indicates thrust type faulting with a very shallow dip angle (11°) (Figure 9). The source time function of the earthquake was determined by the Michigan group (Tanioka and Ruff, 1997) using teleseismic body waves. It shows the total duration of 50 seconds with the

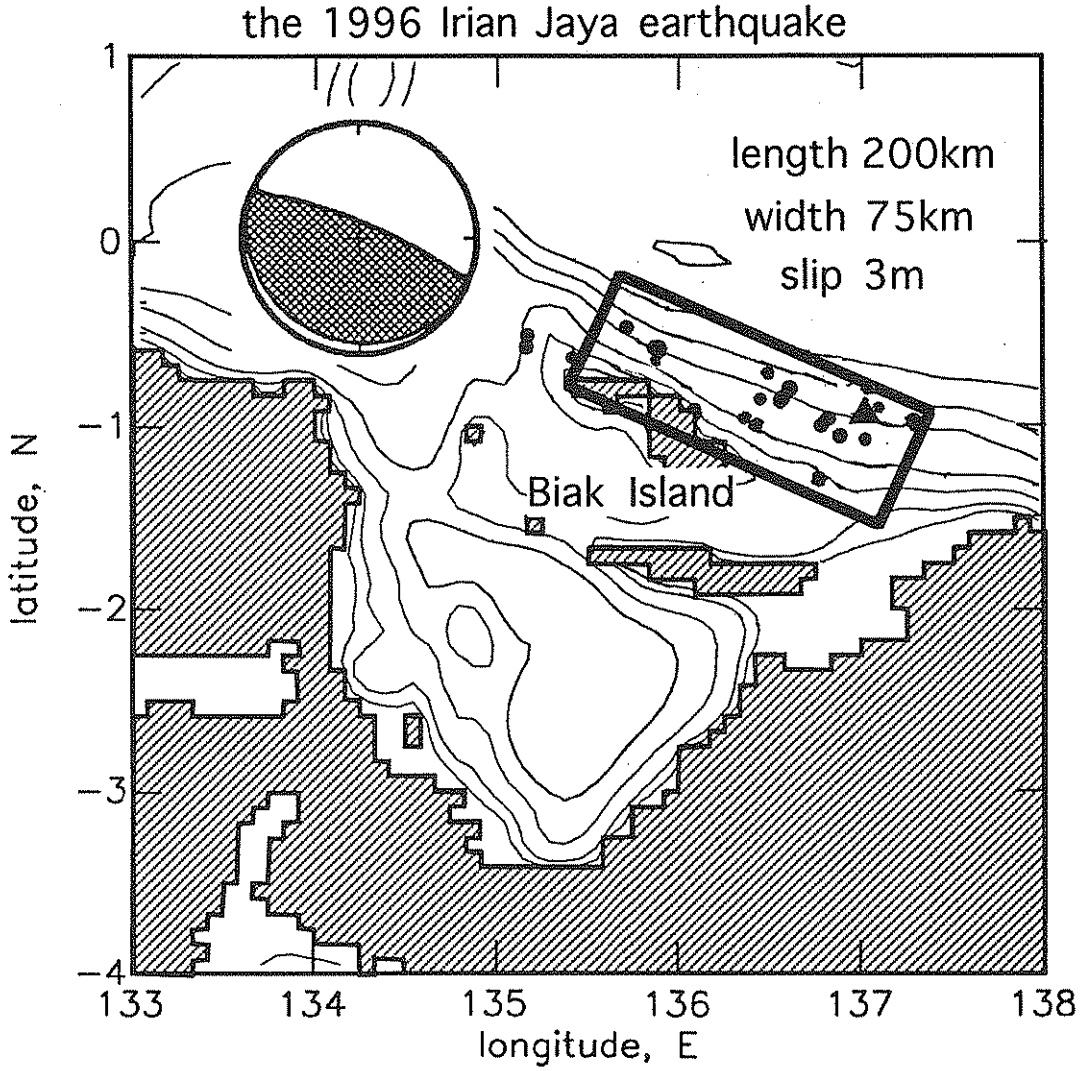

Figure 9. The focal mechanism and the best fault model for the 1996 Irian Jaya earthquake. A flame shows the best fault model. A triangle represents the epicenter of the mainshock. Circles shows the epicenters of the aftershocks.

initial phase of 18 seconds and the seismic moment of 18 X 10^{20} Nm

For this earthquake, we do not have a near-field tsunami waveform recorded at tide gauge. We estimated the fault size (length 200 km, width 75 km) from the aftershock distribution (Figure 10). From the seismic moment of 18 X 10^{20} Nm and a rigidity of 4 X 10^{10} N/m^2, the average slip is calculated to be 3 m.

Tsunamis from the 1996 Irian Jaya earthquake also recorded at tide gauge stations in Japan. We computed the tsunami using a pure thrust type fault (strike=115, dip=10, rake=90) with the above fault size. Figure 10 shows that the observed computed maximum tsunami heights at tide gauge stations in Japan. Overall, the observed and computed maximum tsunami heights shows the good agreements.

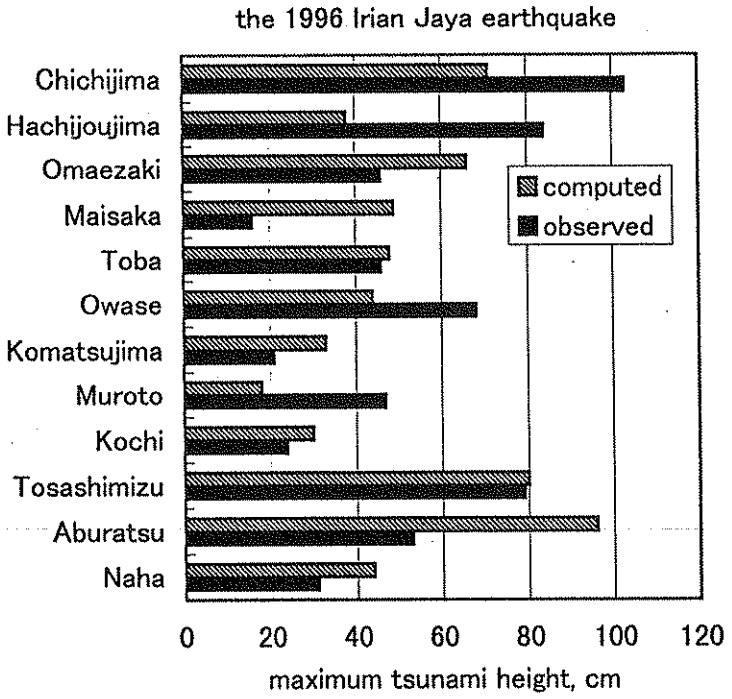

Figure 10. Comparison of the observed and computed maximum tsunami heights at tide gauges in Japan.

6. CONCLUSION

The rupture area of the 1996 Aleutian earthquake is much smaller than the aftershock area. It is located near the epicenter. This indicates that the rupture area of the 1996 Aleutian earthquake did not overlap with the rupture area of the 1986 Andreanov earthquake although the aftershock areas overlaped each other.

Overall, the numerical simulation of the trans-Pacific tsunamis performed well. However, at a few tide gauge station, the difference between the observed and computed maximum tsunami heights was more than factor 2. We still need the improvement of the numerical modeling of trans-Pacific tsunami.

REFERENCE

Ben-Menahem, A. and M. Rosenman, Amplitude pattern of tsunami waves from submarine earthquakes, J. geophy. Res., 77, 3097-3128, 1972

Imamura, F., N.Shuto, and T. Goto, Study of Numerical simulation of the transoceanic propagation; Part 2: Characteristics of tsunami propagating over the Pacific Ocean.

Goto, T., F. Imamura, and N. Shuto, Study of Numerical simulation of the transoceanic propagation of tsunami Part 1, *Jishin 2, 41*, 515-526

Okada, Y., Surface deformation due to shear and tensaile faults in a half space, *Bull. Seism. Soc. Am., 75,*1135-1154, 1985

Ruegg,J.C. et al., The Mw=8.1 Antfagasta (North Chile) earthquake of July 30, 1995: First results from teleseismic and geodetic data, *Geaphys. Res. Lett.*, 1996

Tanioka, Y., and L.J. Ruff, Source time function. Seismo. Res. Lett., (in press).